



IJRASET

International Journal For Research in
Applied Science and Engineering Technology



INTERNATIONAL JOURNAL FOR RESEARCH

IN APPLIED SCIENCE & ENGINEERING TECHNOLOGY

Volume: 12 **Issue:** V **Month of publication:** May 2024

DOI: <https://doi.org/10.22214/ijraset.2024.62138>

www.ijraset.com

Call:  08813907089

E-mail ID: ijraset@gmail.com

Secure Image Sharing: Innovating Encryption and Concealment Methods

Rajeev Keshetty¹, Marineni Tony Dylin², M U Anil Sagar³, Dr. Rishi Sayal⁴

^{1, 2, 3}Research Scholar, ⁴Associate Director, Guru Nanak Institutions Technical Campus, Ibrahimpatnam, Hyderabad

Abstract: Data security techniques, notably concealment of information in encrypted images, play a pivotal role in safeguarding digital assets. Nonetheless, many methods in this domain face challenges in effectively balancing security and embedding capacity. To tackle this issue, we propose a novel approach integrating hybrid coding and Chinese remainder theorem-based secret sharing (CRTSS). Our method employs hybrid coding for concealing data within images, ensuring a robust embedding capacity. Initially, an iterative encryption process encrypts blocks while preserving their spatial correlation. CRTSS is then utilized to distribute these encrypted blocks across multiple shares, ensuring robust security. Leveraging the high geographical correlation within each share, data embedding is performed using the hybrid coding technique, effectively increasing capacity. The proposed method allows for the restoration of the original image without loss, even if some shares are corrupted or missing, as long as enough uncorrupted shares are available. Experimental results indicate superior embedding capacity compared to state-of-the-art techniques, including those relying on secret sharing. We present four variations of the proposed model, comprising two coupled and two separable cases, leading to a high-capacity concealment approach. The efficacy of our approach is demonstrated through experimental validation.

I. INTRODUCTION

The rapid expansion of cloud computing and storage has coincided with the advancement of information technology, particularly with the maturation of 5G communication and transmission. Owing to the benefits of cloud computing, an increasing number of users are storing their information on the cloud, particularly multimedia files like photos, audio snippets, and video files. Since user data is stored on distant or cloud servers or is transferred over public networks, it is not necessarily secure and dependable. As a result, both industry and academics now give considerable attention to the data privacy issue. Numerous strategies exist to safeguard data security, including hashing, data concealing, encryption, and secret sharing (SS). Digital images are important data manifestations that have a wide range of uses in fields like legal forensics, photography, medicine, and the military. One of the areas of research interest is visual data concealing for security protection.

The secret data and cover image are the two things that make up the image data concealment system, as is widely known. To create a stego-picture in an undetectable way, secret data is integrated into the cover image. The picture data hiding mechanism should take into account two circumstances. One is that the cover image is superfluous and the secret data is uniquely safeguarded. Another is that, for military and medical purposes, both the cover picture and the secret data are essential, and both need to be error-free on the decoder side. It is obvious that the latter is reversible data hiding (RDH) and the former is irreversible data hiding. Due to its reversibility, Data Encryption is becoming more and more popular. Data Encryption techniques to date have primarily relied on lossless compression, difference expansion (DE), histogram shifting (HS), and pixel error expansion (PEE). These Data Encryption methods seek to achieve a favorable trade-off between modification distortion and embedding capability.

(1) For Data Encryption, we suggest a hybrid coding. The suggested hybrid coding can surpass the payload restriction of a single coding and obtain a high payload since it combines the benefits of several coding methods.

(2) For data concealing, we create a block-based CRTSS with limitations and a new iterative image encryption. There is greater space for data embedding since repeated encryption can precisely retain spatial correlation. Multiple encrypted shares with good spatial correlations can be produced by the planned CRTSS. Preprocessing is not necessary, and it won't cause data growth.

(3) To create a new Data concealment technique, we take advantage of the suggested hybrid coding, the iterative picture encryption, and the block-based CRTSS with limitations. The suggested approach works better in terms of embedding rate than several cutting-edge Data Concealment techniques, according to experimental results.

The rest of this paper is organized as follows. Section II reviews the related work of popular Data Concealment methods. Section III presents the proposed hybrid coding for Encryption. Section IV illustrates the proposed Data concealment method with secret sharing and hybrid coding in detail. The experimental results are discussed in Section V. Finally, Section VI concludes this paper.

II. RELATED WORK

Numerous Data Concealment techniques have been developed by researchers to date. The current Data Concealment methods can be broadly categorized into four groups: reserving room before encryption (RRBE) [26], [27], [28], [29], [30], [31], [32], [33]; vacating room by encryption (VRBE) [34], [35], [36], [37], [39], [40], [41], [42]; and SS based methods [43], [44], [45], [46], [47], [48], [49]. Together, these four categories comprise the majority of the current Data Concealment methods.

A. VRAE Based Methods

The initial image, which is built on a VRAE framework, was immediately encrypted using conventional image encryption algorithms such stream cipher and the advanced encryption standard (AES) in the early Data Concealment approaches [20], [21], [22], [23], [24], and [25]. The encrypted image in [20] is split up into many chunks. To make room for one hidden bit, the three least significant bits (LSBs) of each block's half pixels are flipped. The original image is simultaneously recovered and secret bits are extracted at the receiver side by using the fluctuation function after the marked image has been directly decrypted. Since then, some advancements in data extraction accuracy have been realized [21], [22]. Since then, some advancements in data extraction accuracy have been realized [21], [22]. Data extraction is not possible in [20], [21], and [22] when the encryption key is not provided. More adaptably, Zhang [23] and Qian and Zhang [24] suggested separable techniques that involve compressing some LSB planes of the stream cipher encrypted image to make more space for data embedding. In this way, data extraction becomes independent of picture recovery and the encryption key. To achieve data concealment, some randomly selected pixels from the stream cipher encrypted image are changed with secret bits in [25] in place of their high bit-planes. Since there are two possible outcomes for a single high bit-plane, "0" and "1," the prediction errors produced by these two outcomes are compared in order to recover the original image.

B. RRBE Based Methods

Despite the stream cipher's strong performance in picture encryption, the loss of pixel spatial correlation makes it challenging to remove an embedding room directly from the encrypted image. Consequently, a few RRBE-based strategies were put forth to help achieve large payloads [26], [27], [28], [29], [30], [31], [32], and [33]. In order to free up space before picture encryption, Ma et al. [26] integrated a few LSBs of the texture area into the smooth area using the conventional RDH technique. Secret data is included in the released room. The patch-level sparse representation method is employed in [27] to significantly reduce the amount of space in the original image. A binary-block embedding (BBE) technique was suggested by A binary-block embedding (BBE) technique was proposed by Yi and Zhou [28]. BBE is used to embed the original image's lower bit-planes into its upper bit-planes, freeing up the lower bit-planes for data hiding. The most important bits (MSBs) were rearranged by Chen and Chang [29] to construct bitstreams, which were then effectively compressed to provide the embedding room. In [30], the same high bit-planes that are successively labeled are compared between the original pixel and its predicted value. Secret bits are stored on the bit-planes with labels. In [31], secret bits are embedded into the embeddable bit-planes in accordance with the labels generated by hierarchically dividing the prediction errors into three magnitudes. In Yin et al. [32], To obtain a high embedding capacity, Yin et al. [32] employed pixel prediction and compressed the high bit-planes of prediction errors. In order to evacuate the huge room prior to encryption, an adaptive L predictor for preprocessing is constructed in Mohammadi's [33] general RRBE framework for Data Concealment.

C. VRBE Based Methods

Although RRBE-based techniques provide outstanding embedding performance, their practical applicability may be limited because the content owner lacks the computational capacity to undertake pretreatment operations or is unaware that the following data is hidden. Some particular encryption-based techniques, especially VRBE-based techniques, were presented to overcome this problem. The encrypted image in [34], [35], and [36] is produced by block permutation and block-based bit-XOR, both of which are capable of maintaining the correlation inside each encrypted block. Next, data concealing is accomplished by using difference compression [36], adaptive block encoding [35], and difference histogram shifting (DHS) [34]. The original image is encrypted in [37] and [38] by using block permutation and disordering bit planes, which transfers the redundant space from the original image to the encrypted image. To remove space for data concealment, high bit-plane portions of the encrypted image are compressed using efficient sparse coding. In order to maintain spatial correlations among image blocks, Yi and Zhou [39] first encrypted the original image using block permutation and block-based modulation. They then used parametric binary tree labeling (PBTL) to insert secret data into the encrypted image. In [40], redundancy is preserved in the encrypted image by employing the CE technique, which encrypts the original image in chunks using the stream cipher.

Subsequently, the redundancy matrix format is employed to free up space for data embedding. In order to obtain high embedding capacity, Yu et al. [41] presented an adaptive difference recovery (ADR) based data hiding technique and subsequently implemented this technique in Data Concealment. A generalized methodology for high-capacity Data Concealment utilizing pixel prediction and entropy encoding was presented by Qiu et al. [42] and is applicable to both the RRBE and VRBE scenarios.

D. SS Based Methods

An original image is converted into an encrypted version and uploaded to the cloud using the Data Concealment techniques mentioned above. Attacks by a third party could compromise the encrypted image and result in incorrect image recovery on the recipient's end. Some secret sharing (SS) based Data Concealment techniques were proposed [43], [44], [45], [46], [47], [48], and [49] in an effort to increase the robustness of RDHEI. Wu et al. [43] used pairwise Shamir's SS [10] to encrypt the original image in order to create the encrypted shares, ensuring that each share's pixel pair difference is equal to that of the original pair. Secret data can be integrated into shares using the DE or DHS technique because of difference preservation. Another SS was proposed by Chen et al. [44]. Another SS-based Data Concealment technique was proposed by Chen et al. [44]. This method encrypts a pair of pixels using a degree 3 polynomial after preprocessing them using the DE technique. The encrypted pixel pair may contain one secret bit inserted in it. One data-hider does the data concealing in [43] and [44].

The original image might not be recovered in the case that the data hider is an attacker for the original image since it might be an unreliable third party. Some multiple data-hiders based Data Concealment approaches using SS were presented [45], [46], [47], [48], and [49] to address this problem. These methods distribute each share to a single data-hider and provide independent data hiding on each share. Two Data Concealment techniques via SS over Galois fields GF(p) and GF(28) were proposed by Qin et al. [45]. These two techniques allow the embedding room to be abandoned in each share by preserving the pixel disparities within the 2x2 blocks of each share after SS. Multiple data-hiders get the encrypted shares in [46], which are produced using a particular Shamir's SS [10]. Through the bit-plane substitution approach, each data hider incorporates secret data into their share. Because Shamir's SS is often built on a finite field Fp with prime size 251, it is not possible to communicate pixels with values larger than 251. Accordingly, in these Shamir's SS based algorithms [43], [44], [45], and [46], the pixels with values more than 251 are preprocessed. CRTSS [8] is used in [47] to encrypt the original image and produce several shares. The additive homomorphism of CRT and the DE method are used in each share to hide data. Pixel enlargement arises from the use of CRTSS [8] and needs to be solved by compressing two MSBs of each share using this method. Because the DE approach is used, this method's embedding capacity is not high, hovering around 0.5 bpp. First presented by Hua et al. [48], cipher-feedback secret sharing (CFSS) is a technique that can be used to share images. An approach called multi-MSB prediction is used to hide data. Using matrix theory, Hua et al. [49] originally presented a matrix-based secret sharing (MSS). To attain a high payload, they subsequently suggested an MSS-RDHEI approach utilizing block error mixture encoding (BEME).

In essence, these high-payload Data Concealment methods nearly take use of certain coding strategies to represent the image context with less information, freeing up space for secret data like BEME [49], PBTL [39], and entropy encoding [42]. These single-coding methods can yet be improved upon, even though they can yield a large payload. In order to introduce a novel Data Concealment approach, we suggest in this study a hybrid coding with a bigger payload.

III. METHODOLOGIES

A. Proposed Hybrid Coding for RDH

Here, we provide a hybrid coding scheme for data hiding. Entropy coding and hierarchical coding make up the hybrid coding method. Blocks are used to separate an image. Every block is encoded using either hierarchical or entropy coding. Additionally, the block is encoded using the coding technique that has more free space so that the embedding capacity is increased.

Assume that I is the original, 8-bit grayscale image with a size of H×W. First, the original image I is separated into n non-overlapping blocks, denoted by the numbers B1, B2,..., and Z, which are scanned in raster order. Every block has a t×t dimensions. The formula $z = \lfloor H/t \rfloor \times \lfloor W/t \rfloor$ is evident. The prediction value of a block's pixel $p_{i,j}$ is determined as

$$\bar{p}_{i,j} = \begin{cases} a, & \text{if } i = 1 \text{ and } j \geq 2 \\ b, & \text{if } i \geq 2 \text{ and } j = 1 \\ \max(a,b), & \text{if } 2 \leq i, j \leq t \text{ and } c \leq \min(a,b) \\ \min(a,b), & \text{if } 2 \leq i, j \leq t \text{ and } c \geq \max(a,b) \\ b + a - c, & \text{Otherwise} \end{cases} \quad (1)$$

in where $b = p(i-1, j)$, $c = p(i-1, j-1)$, and $a = p(i, j-1)$. [55]

The median edge detector (MED) predicts the remaining pixels, while the preorder pixels of the first row or column anticipate the remaining pixels. Keep in mind that the reference pixel, $p_{1,1}$, is not included in the data concealing. Following that, the prediction error (PE) is produced by[55]

$$e_{i,j} = \tilde{p}_{i,j} - p_{i,j} \tag{2}$$

Each block's PEs are computed using Equation (2), and they are then converted into the one-dimensional PE sequence $e = [e_2, e_3, \dots, e_f]$ ($f = t \times t$) in the order shown in Figure 1. The PEs' indexes in the one-dimensional sequence are represented by the numbers in Fig. 1. The entire image can then be obtained as a PE sequence, $PE = \{e_1, e_2, \dots, e_z\}$, with a dimension of $(t \times t - 1) \times z$. Next, each block is encoded using the hierarchical and entropy coding methods, respectively. The block is encoded using the coding scheme that has more free space. The following is an illustration of these two coding strategies.

$p_{i,t}$	0	1	2
3	6	7	8
4	9	10	11
5	12	13	14

Fig. 1: Scan Order[55]

B. Hierarchical Coding

The hierarchical coding in this part is done in a single block. As an example, we consider a single block and its PEs. In the PE sequence $[|e_2|, |e_3|, \dots, |e_f|]$, let m_e be the maximum element. m_e is first divided into three categories in [41]: $m_e = 0$, $0 < m_e < 64$, and $m_e \geq 64$. This block is designated $l = 0$ and all of the block's pixels, with the exception of $p_{1,1}$, can hold eight secret bits if $m_e = 0$. A secret bit cannot be inserted into this block if m_e is less than 64. This block is designated by $l = 7$. It is split hierarchically into a set of nodes when $0 < m_e < 26$. The root node $0 < m_e < 26$ is split into three nodes, $0 < m_e < 25$, $m_e = 25$, and $25 < m_e < 26$, as illustrated in Fig. 2. $0 < m_e < 2q-1$, $m_e = 2q-1$, and $2q-1 < m_e < 2q$ make up the three nodes that make up the left node, $0 < m_e < 2q$. Every layer is associated with a specific bit of the pixel; for example, the $(q + 1)$ th bit corresponds to the $(8 - q)$ th layer. Which layer m_e is on is determined by the leaf node. The block label is considered to represent the layer index. In [41], the block label is $l = 8 - q - 1$, where $1 \leq q \leq 6$. If $2q-1 < m_e < 2q$, m_e returns to the left node $0 < m_e < 2q$ of the higher layer as the red arrow depicted in Fig. 2. With the exception of $p_{1,1}$, all pixels' $(q + 2)$ th ~ 8th bits can hold $8 - q - 1$ secret bits. Consequently, the payload of this block is as follows when m_e is situated on the left node $0 < m_e < 2q$ of the $(8 - q - 1)$ th layer:

$$EC = (f - 1) \times (8 - q - 1) \tag{3}$$

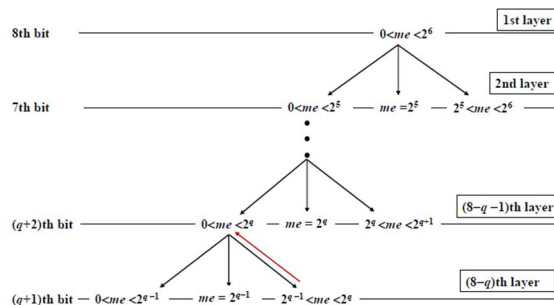


Fig. 1. Hierarchical Structure.[55]

In this work, the payload gain determines whether m_e with $2q-1 < m_e < 2q$ returns the upper layer or not. For each $|e_i| (2 \leq i \leq f)$ in the block where $2q-1 < m_e < 2q$, there are three possible outcomes: $|e_i| \in [0, 2q-1]$, $|e_i| = 2q-1$, and $|e_i| \in [2q-1+1, 2q-1]$; these three situations can hold $8-q$, $8-q-1$, and $8-q$ secret bits, respectively, in accordance with the approach [31]. It is evident that $l=8-q$ is the block label. To keep things simple, we will refer to the PEs with the numbers n_0, n_1, n_2 , and n_3 as C_0, C_1, C_2 , and C_3 , respectively, and the expressions $|e_i|=0$, $|e_i| \in [1, 2q-1]$, $|e_i|=2q-1$, and $|e_i| \in [2q-1+1, 2q-1]$. As illustrated in Fig. 2, when m_e with $2q-1 < m_e < 2q$ is situated on the $(8-q)$ th layer, the block's payload is

$$ECp = (8 - q) \times (n_0 + n_1 + n_3) + n_2 \times (8 - q - 1) \quad (4)$$

where $n_0 + n_1 + n_2 + n_3 = f - 1$. [55]

It is important to note that C2's payload is the same whether it is in the $(8 - q - 1)$ th layer or the $(8 - q)$ th layer. Consequently, in contrast to the $(8 - q - 1)$ th layer, the block's $(8 - q)$ th layer's payload gain is

$$ECg = ECp - EC = n_0 + n_1 + n_3 \quad (5)$$

when $2^{q-1} < me < 2^q$. [55]

When me with $2^{q-1} < me < 2^q$ is found on the $(8 - q)$ th layer, the payload of this block can be enhanced; however, more information is needed to differentiate between C1 and C3 during data extraction and image recovery. It should be noted that during data extraction and picture recovery—discussed in Section D—C0 and C2 can be adaptively determined.

The layer on which me is located is determined by calculating the pure payload gain, which is used to improve the block's pure payload. As $2^{q-1} < me < 2^q$ allows for the adaptive determination of C0 and C2, the only thing left to do is differentiate between C1 and C3. Generally speaking, there are fewer C3s than C1s. To store the index of every C3 in $[|e2|, |e3|, \dots, |ef|]$, more bits are needed. It is possible to determine the index of C1 after determining the index of C3. First, in order to record the value of n_3 , $\lceil \log_2(t \times t - 1) \rceil$ bits are needed. Next, we record each C3's index using the variable bit length. Assume that each C3 has a location index value of $\{x_i\}_{n_3, i=1}^{(0 \leq x_i \leq f-2)}$. Then, each C3's index can be expressed in terms of r_i bits, which are computed as follows. [55]

$$r_i = \begin{cases} \lceil \log_2(f - 1) \rceil, & \text{if } i = 1 \\ \max\{\log_2(f - 1 - x_{i-1}), 1\}, & \text{if } 2 \leq i \leq n_3 \end{cases} \quad (6)$$

As a result, the index information length of C3 in a block is determined as [55]

$$le = \lceil \log_2(t \times t - 1) \rceil + \sum_{i=1}^{n_3} r_i \quad (7)$$

Le bits can be used to encode the index information of C3 in the way described above. As such, the block label is produced by [55]

$$l = \begin{cases} 8 - q - 1, & \text{if } ECg \leq le \\ 8 - q, & \text{if } ECg > le \end{cases} \quad (8)$$

In this case, $1 \leq l \leq 6$. When me with $2^{q-1} < me < 2^q$ is positioned on the $(8 - q)$ th layer, $ECg \leq le$ indicates that there is no yield on payload. And I ought to give back the top layer, which is the $(8 - q - 1)$ th layer. This block's payload, EC , is determined by using Equation (3). In accordance with this, the block label is $8 - q - 1$. The block label is $8 - q$ and the payload may be computed using Eq. (4) if $ECg > le$. $PEC = ECg - le > 0$ represents the pure payload benefit. Subsequently, since $0 \leq l < 7$, the block label l is divided into three bits. Furthermore, an additional bit $b_{add} = 1$ indicates that me is subject to $2^{q-1} < me < 2^q$ when it is positioned on the $(8 - q)$ th layer. Furthermore, if me is on the $(8 - q)$ th layer, more bits $b_{add} = 1$ mean that me is subject to $2^{q-1} < me < 2^q$, and more bits $b_{add} = 0$ mean that me is susceptible to $0 < me < 2^{q-1}$ or $me = 2^{q-1}$. To capture the index information of C3 for $0 < me < 2^{q-1}$ or $me = 2^{q-1}$, it is evident that no bits are needed.

The detailed encoding information for several scenarios when the original image is an 8-bit gray-level image is shown in Fig. 3. The block label bits include the encoding information for the block with $l = 0, l = 7$, or $l = 1$. The block label bits include the encoding information for the block with $l = 0, l = 7$, or $l = 1$. The block label bits, an extra bit $b_{add} = 1$, and the index information of C3 make up the encoding information for the block with $2 \leq l \leq 6$, or in this work, the block label bits and an additional bit $b_{add} = 0$. Ultimately, the block's embedding capacity produced via hierarchical coding is determined by [55]

$$EC_{hier} = \begin{cases} 8 \times (t \times t - 1) - 3, & \text{if } l = 0 \\ 0 - 3, & \text{if } l = 7 \\ t \times t - 1 - 3, & \text{if } l = 1 \\ ECp - 4, & \text{if } 2 \leq l \leq 6 \text{ and } b_{add} = 0 \\ ECp - le - 4, & \text{if } 2 \leq l \leq 6 \text{ and } b_{add} = 1 \end{cases} \quad (9)$$

where Eqs. (4) and (7) can be used to yield EC_p and l_e, respectively, for l = 8 - q. Given that there are no PEs with C3, take note that n₃ = 0 if badd = 0 in Eq. (4).

l=0, m=0	0 0 0 0	Block label bits
l=7, m=264	1 1 1 1	The bit representing the range of m
l=1, 0<m<64	0 0 0 1	Index information of C ₃
l=2, 0<m<32	0 0 0 0 0	$\lceil \log_2(r-1) \rceil$ $\sum_{i=1}^{n_3} r_i$
l=2, 32<m<64	0 0 0 1 1	
l=3, 0<m<16	0 0 0 0 0	
l=3, 16<m<32	0 0 0 1 1	
l=4, 0<m<8	0 0 0 0 0	
l=4, 8<m<16	0 0 0 1 1	
l=5, 0<m<4	0 0 0 0 0	
l=5, 4<m<8	0 0 0 1 1	
l=6, 1<m<2	0 0 0 0 0	
l=6, m=3	0 0 0 1 1	

Fig. 3: Hierarchical encoding information[55]

C. Entropy coding

Huffman and arithmetic coding are two popular lossless entropy coding methods. The codewords and symbols in Huffman coding correspond exactly to one another. Thus, for every block, we compute the embedding capacity using Huffman coding. First, we compress the image's PEs using Huffman coding. $\{e_1, e_2, \dots, e_z\}$ is the PE. The codewords $c(-255), c(-254), \dots, c(254), c(255)$ formed using Huffman coding, whose length are $len(-255), len(-254), \dots, len(254), len(255)$, are obtained since the PE falls within the range of $[-255, 255]$. Next, we may determine one block B's Huffman encoding information's length by[55]

$$len_{huff} = \sum_{i=2}^f len(e_i) \tag{10}$$

The embedding capacity of one block generated by Huffman coding is derived by[55]

$$EC_{huff} = 8 \times (t \times t - 1) - len_{huff} \tag{11}$$

D. Data embedding using hybrid coding

Blocks inside the designated image are separated in raster scanning sequence. In case the LSBs of the initial pixels $\{p_{1,1}\}$ are "0," the blocks are gathered. With the exception of the first pixel, each pixel in these blocks is converted into a binary sequence that contains embedded data and auxiliary information. It is evident that the substituted LSBs, entropy encoding information, and hierarchical encoding information make up the auxiliary information. The first pixel of each block can be retrieved as $p_{1,1}$ with the new LSBs. Decoding the entropy encoding information yields the blocks that start with "0." Subsequently, the blocks containing the number "1" can have their remaining embedded data retrieved and recovered using the hierarchical coding information.

IV. PROPOSED DATA CONCEALMENT METHOD WITH SECRET SHARING AND HYBRID CODING

The suggested Data Concealment method's framework, which includes data concealing, data exaction and picture recovery, and iterative encryption and image sharing, is shown in Fig. 6. To further security, the content owner uses iterative encryption to create an encrypted image. This encrypted image is then shared via block-based CRTSS, and several encrypted shares are sent to multiple data hiders. He or she can use hybrid coding to separately perform Data Encryption at each data-hider side. Using CRTSS, the original image can be retrieved without loss once the shareholders have provided enough marked encrypted shares.

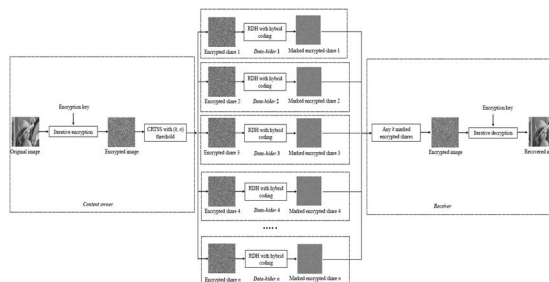


Fig. 6: Framework of the proposed data concealment method[55]

ABE System Algorithm:

AES – Encryption and Decryption Specification

The image can only be viewed by the receiver as the image is encrypted using AES and the key is only known to the sender and receiver. Since the image is encrypted using AES, it is more secure than the DES and triple DES.

AES is called AES-128, AES-192 and AES-256. This classification depends on the different key size used for cryptographic process. Those different key sizes are used to increase the security level. As, the key size increases the security level increases. Hence, key size is directly proportional to the security level. The input for AES process is a single block of 128 bits. The processing is carried out in several number of rounds where it depends on the key length: 16 byte key consists of 10 rounds, 24 byte key consists of 12 rounds, and 32 byte key consists of 14 rounds. The first round of encryption process consists of four distinct transformation functions:

- Substitution Bytes
- ShiftRows
- MixColumns
- AddRoundKey
- The final round consists of only three transformation ignoring MixColumns. The Decryption method is the reverse of encryption and it consists of four transformations [4].
- Inverse Substitution Bytes
- Inverse ShiftRows
- Inverse MixColumns
- AddRoundKey
- Setup (λ , U): The setup algorithm takes as input a security parameter and attribute universe U, and outputs a master secret key MSK and the public parameters PP.
- Encrypt (PP, A, M): The encryption algorithm takes as input the public parameters PP, an access structure A and a message M, and outputs a ciphertext CT.
- KeyGen (MSK, S): The key generation algorithm takes as input the master secret key MSK and an attribute set S, and outputs a secret key SK.
- Decrypt (PP, SK): The decryption algorithm takes as input the public parameters PP, a secret key SK.

SnapShots

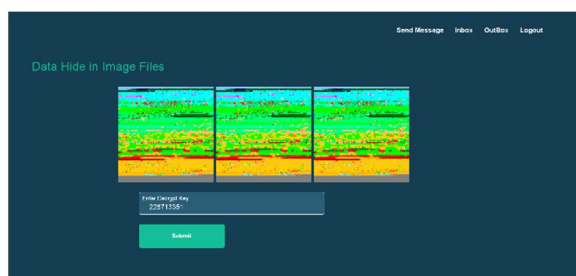


Fig4.1: Process of iterative encryption

Explanation: The figure 4.1 describes about the steps of iterative encryption of the Image in the data hider page

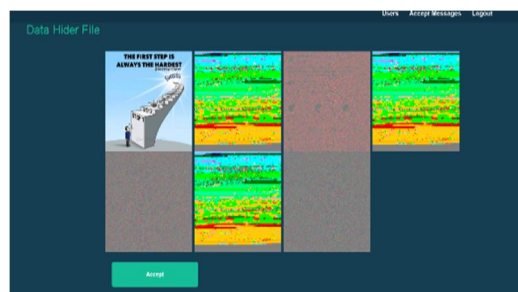


Fig 4.2: Process of Decryption

Explanation: The fig 4.2 describes about the process of decryption on the receiver side using the decryption key.

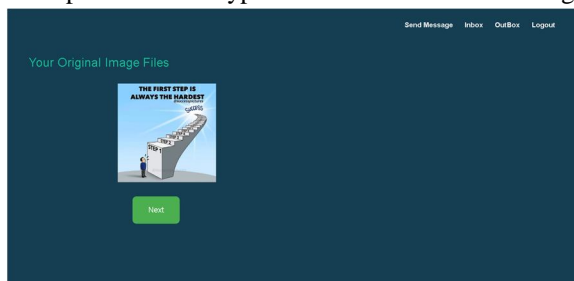


Fig 4.3 : The original Image after Decryption

Explanation: The fig 4.3 shows the original image decrypted on the receiver side .

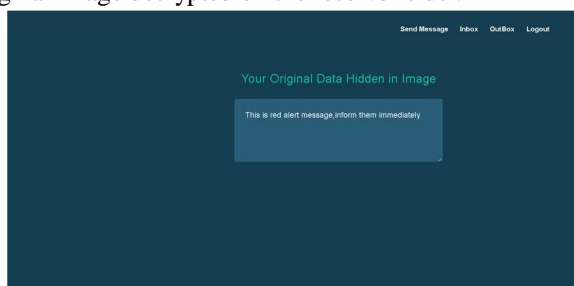


Fig 4.4: The message hidden in the image

Explanation: The fig 4.4 shows the message hided in the image ,this will be appeared after decrypting the image on the receiver side

V. CONCLUSION AND FUTURE ENHANCEMENT

Our innovative Data Concealment technique makes use of hybrid coding and secret sharing. A substantial embedding room for each encrypted share can be achieved by the suggested method's combination of block-based CRTSS and iterative encryption, which can effectively pervert correlations within the blocks. Hybrid coding is used in each encrypted exchange to hide data with a large payload. Furthermore, the suggested approach does not call either pre-processing or pixel extension. According to experimental findings, the suggested approach performs better in the payload than a few cutting-edge SS-based Data Concealment techniques.

Future Work: Future research will look into how to use the suggested model in additional scenarios, including a combined Data Encryption in images. Expanding the concept of secret sharing to include other forms of multimedia, including audio and video, is also an intriguing avenue to pursue.

REFERENCES

- [1] Y. Du, Z. Yin, and X. P. Zhang, "High capacity lossless data hiding in jpeg bit stream based on general vlc mapping," *IEEE Transactions on Dependable and Secure Computing*, vol. 19, no. 2, pp. 1420–1433, 2022.
- [2] Z. Wang, G. Feng, L. Shen, and X. Zhang, "Cover selection for steganography using image similarity," *IEEE Transactions on Dependable and Secure Computing*, pp. 1–13, 2022.
- [3] Y. Xian, X. Wang, and L. Teng, "Double parameters fractal sorting matrix and its application in image encryption," *IEEE Transactions on Circuits and Systems for Video Technology*, vol. 32, no. 6, pp. 4028–4037, 2022.
- [4] X. Wang and S. Gao, "Image encryption algorithm for synchronously updating boolean networks based on matrix semi-tensor product theory," *Information sciences*, vol. 507, pp. 16–36, 2020.
- [5] Z. Tang, L. Chen, X. Q. Zhang, and S. Zhang, "Robust image hashing with tensor decomposition," *IEEE Transactions on Knowledge and Data Engineering*, vol. 31, no. 3, pp. 549–560, 2019.
- [6] X. Liang, Z. Tang, J. Wu, Z. Li, and X. P. Zhang, "Robust image hashing with is map and saliency map for copy detection," *IEEE Transactions on Multimedia*, pp. 1–1, 2021.
- [7] X. Liang, Z. Tang, Z. Huang, X. Q. Zhang, and S. Zhang, "Efficient hashing method using 2D-2D PCA for image copy detection," *IEEE Transactions on Knowledge and Data Engineering*, pp. 1–1, 2021.
- [8] C. Asmuth and J. Bloom, "A modular approach to key safeguarding," *IEEE transactions on information theory*, vol. 29, no. 2, pp. 208–210, 1983.
- [9] X. Yan, Y. Lu, L. Liu, and X. Song, "Reversible image secret sharing," *IEEE Transactions on Information Forensics and Security*, vol. 15, pp. 3848–3858, 2020.
- [10] A. Shamir, "How to share a secret," *Communications of the ACM*, vol. 22, no. 11, pp. 612–613, 1979.

- [11] X. Yan, Y. Lu, C.-N. Yang, X. Zhang, and S. Wang, "A common method of share authentication in image secret sharing," *IEEE Transactions on Circuits and Systems for Video Technology*, vol. 31, no. 7, pp. 2896–2908, 2021.
- [12] J. Tian, "Reversible data embedding using a difference expansion," *IEEE transactions on circuits and systems for video technology*, vol. 13, no. 8, pp. 890–896, 2003.
- [13] Z. Ni, Y.-Q. Shi, N. Ansari, and W. Su, "Reversible data hiding," *IEEE Transactions on circuits and systems for video technology*, vol. 16, no. 3, pp. 354–362, 2006.
- [14] W. Zhang, X. Hu, X. Li, and N. Yu, "Recursive histogram modification: establishing equivalency between reversible data hiding and lossless data compression," *IEEE transactions on image processing*, vol. 22, no. 7, pp. 2775–2785, 2013.
- [15] W. Zhang, X. Hu, X. Li, and Y. Nenghai, "Optimal transition probability of reversible data hiding for general distortion metrics and its applications," *IEEE Transactions on Image Processing*, vol. 24, no. 1, pp. 294–304, 2014.
- [16] C. Yu, X. Q. Zhang, D. Wang, and Z. Tang, "Reversible data hiding with pairwise PEE and 2D-PEH decomposition," *Signal Processing*, vol. 196, p. 108527, 2022.
- [17] D. Wang, X. Q. Zhang, C. Yu, and Z. Tang, "Reversible data hiding by using adaptive pixel value prediction and adaptive embedding bin selection," *IEEE Signal Processing Letters*, vol. 26, no. 11, pp. 1713–1717, 2019.
- [18] W. Puech, M. Chaumont, and O. Strauss, "A reversible data hiding method for encrypted images," in *Security, forensics, steganography, and watermarking of multimedia contents X*, vol. 6819, p. 68191E, International Society for Optics and Photonics, 2008.
- [19] P. Puteaux and W. Puech, "An efficient msb prediction-based method for high-capacity reversible data hiding in encrypted images," *IEEE Transactions on Information Forensics and Security*, vol. 13, no. 7, pp. 1670–1681, 2018.
- [20] X. P. Zhang, "Reversible data hiding in encrypted image," *IEEE signal processing letters*, vol. 18, no. 4, pp. 255–258, 2011.
- [21] W. Hong, T.-S. Chen, and H.-Y. Wu, "An improved reversible data hiding in encrypted images using side match," *IEEE Signal Processing Letters*, vol. 19, no. 4, pp. 199–202, 2012.
- [22] X. Liao and C. Shu, "Reversible data hiding in encrypted images based on absolute mean difference of multiple neighboring pixels," *Journal of Visual Communication and Image Representation*, vol. 28, pp. 21–27, 2015.
- [23] X. P. Zhang, "Separable reversible data hiding in encrypted image," *IEEE transactions on information forensics and security*, vol. 7, no. 2, pp. 826–832, 2011.
- [24] Z. Qian and X. P. Zhang, "Reversible data hiding in encrypted images with distributed source encoding," *IEEE Transactions on Circuits and Systems for Video Technology*, vol. 26, no. 4, pp. 636–646, 2015.
- [25] X. Wu and W. Sun, "High-capacity reversible data hiding in encrypted images by prediction error," *Signal processing*, vol. 104, pp. 387–400, 2014.
- [26] K. Ma, W. Zhang, X. Zhao, N. Yu, and F. Li, "Reversible data hiding in encrypted images by reserving room before encryption," *IEEE Transactions on information forensics and security*, vol. 8, no. 3, pp. 553–562, 2013.
- [27] X. Cao, L. Du, X. Wei, D. Meng, and X. Guo, "High capacity reversible data hiding in encrypted images by patch-level sparse representation," *IEEE transactions on cybernetics*, vol. 46, no. 5, pp. 1132–1143, 2016.
- [28] S. Yi and Y. Zhou, "Binary-block embedding for reversible data hiding in encrypted images," *Signal Processing*, vol. 133, pp. 40–51, 2017.
- [29] K. Chen and C.-C. Chang, "High-capacity reversible data hiding in encrypted images based on extended run-length coding and block-based msb plane rearrangement," *Journal of Visual Communication and Image Representation*, vol. 58, pp. 334–344, 2019.
- [30] Z. Yin, Y. Xiang, and X. P. Zhang, "Reversible data hiding in encrypted images based on multi-msb prediction and huffman coding," *IEEE Transactions on Multimedia*, vol. 22, no. 4, pp. 874–884, 2020.
- [31] C. Yu, X. Q. Zhang, X. P. Zhang, G. Li, and Z. Tang, "Reversible data hiding with hierarchical embedding for encrypted images," *IEEE Transactions on Circuits and Systems for Video Technology*, vol. 32, no. 2, pp. 451–466, 2022.
- [32] Z. Yin, Y. Peng, and Y. Xiang, "Reversible data hiding in encrypted images based on pixel prediction and bit-plane compression," *IEEE Transactions on Dependable and Secure Computing*, vol. 19, no. 2, pp. 992–1002, 2022.
- [33] A. Mohammadi, "A general framework for reversible data hiding in encrypted images by reserving room before encryption," *Journal of Visual Communication and Image Representation*, vol. 85, p. 103478, 2022.
- [34] F. Huang, J. Huang, and Y.-Q. Shi, "New framework for reversible data hiding in encrypted domain," *IEEE transactions on information forensics and security*, vol. 11, no. 12, pp. 2777–2789, 2016.
- [35] Y. Fu, P. Kong, H. Yao, Z. Tang, and C. Qin, "Effective reversible data hiding in encrypted image with adaptive encoding strategy," *Information Sciences*, vol. 494, pp. 21–36, 2019.
- [36] Z. Tang, S. Xu, H. Yao, C. Qin, and X. Q. Zhang, "Reversible data hiding with differential compression in encrypted image," *Multimedia Tools and Applications*, vol. 78, no. 8, pp. 9691–9715, 2019.
- [37] Z. Liu and C. Pun, "Reversible data-hiding in encrypted images by redundant space transfer," *Information Sciences*, vol. 433, pp. 188–203, 2018.
- [38] C. Qin, X. Qian, W. Hong, and X. P. Zhang, "An efficient coding scheme for reversible data hiding in encrypted image with redundancy transfer," *Information Sciences*, vol. 487, pp. 176–192, 2019.
- [39] S. Yi and Y. Zhou, "Separable and reversible data hiding in encrypted images using parametric binary tree labeling," *IEEE Transactions on Multimedia*, vol. 21, no. 1, pp. 51–64, 2019.
- [40] Z. Liu and C. Pun, "Reversible data hiding in encrypted images using chunk encryption and redundancy matrix representation," *IEEE Transactions on Dependable and Secure Computing*, vol. 19, no. 2, pp. 1382–1394, 2022.
- [41] C. Yu, X. Q. Zhang, G. Li, S. Zhan, and Z. Tang, "Reversible data hiding with adaptive difference recovery for encrypted images," *Information Sciences*, vol. 584, pp. 89–110, 2022.
- [42] Y. Qiu, Q. Ying, Y. Yang, H. Zeng, S. Li, and Z. Qian, "High-capacity framework for reversible data hiding in encrypted image using pixel prediction and entropy encoding," *IEEE Transactions on Circuits and Systems for Video Technology*, vol. 32, no. 9, pp. 5874–5887, 2022.
- [43] X. Wu, J. Weng, and W. Yan, "Adopting secret sharing for reversible data hiding in encrypted images," *Signal Processing*, vol. 143, pp. 269–281, 2018.
- [44] Y. Chen, T. Hung, S. Hsieh, and C. Shiu, "A new reversible data hiding in encrypted image based on multi-secret sharing and lightweight cryptographic algorithms," *IEEE Transactions on Information Forensics and Security*, vol. 14, no. 12, pp. 3332–3343, 2019.



- [45] C. Qin, C. Jiang, Q. Mo, H. Yao, and C. Chang, "Reversible data hiding in encrypted image via secret sharing based on GF (p) and GF (28)," *IEEE Transactions on Circuits and Systems for Video Technology*, vol. 32, no. 4, pp. 1928–1941, 2022.
- [46] B. Chen, W. Lu, J. Huang, J. Weng, and Y. Zhou, "Secret sharing based reversible data hiding in encrypted images with multiple data-hiders," *IEEE Transactions on Dependable and Secure Computing*, vol. 19, no. 2, pp. 978–991, 2022.
- [47] Y. Ke, M. Zhang, X. P. Zhang, J. Liu, T. Su, and X. Yang, "A reversible data hiding scheme in encrypted domain for secret image sharing based on chinese remainder theorem," *IEEE Transactions on Circuits and Systems for Video Technology*, vol. 32, no. 4, pp. 2469–2481, 2022.
- [48] Z. Hua, Y. Wang, S. Yi, Y. Zhou, and X. Jia, "Reversible data hiding in encrypted images using cipher-feedback secret sharing," *IEEE Transactions on Circuits and Systems for Video Technology*, vol. 32, no. 8, pp. 4968–4982, 2022.
- [49] Z. Hua, Y. Wang, S. Yi, Y. Zheng, X. Liu, Y. Chen, and X. Zhang, "Matrix-based secret sharing for reversible data hiding in encrypted images," *IEEE Transactions on Dependable and Secure Computing*, 2022.
- [50] L. Qu, F. Chen, S. Zhang, and H. He, "Cryptanalysis of reversible data hiding in encrypted images by block permutation and co-modulation," *IEEE Transactions on Multimedia*, vol. 24, pp. 2924–2937, 2021.
- [51] L. Qu, H. He, and F. Chen, "On the security of block permutation and coxor in reversible data hiding," *IEEE Transactions on Circuits and Systems for Video Technology*, vol. 32, no. 3, pp. 920–932, 2022.
- [52] P. Bas, T. Filler, and T. Pevn' y, "Break our steganographic system: The ins and outs of organizing boss," in *International workshop on information hiding*, pp. 59–70, Springer, 2011.
- [53] P. Bas and T. Furon, "Image database of bows-2," Accessed: Jun, vol. 20, 2017.
- [54] G. Schaefer and M. Stich, "Ucid: An uncompressed color image database," in *Storage and Retrieval Methods and Applications for Multimedia 2004*, vol. 5307, pp. 472–480, International Society for Optics and Photonics, 2003.
- [55] C. Yu, X. Zhang, C. Qin and Z. Tang, "Reversible Data Hiding in Encrypted Images With Secret Sharing and Hybrid Coding," in *IEEE Transactions on Circuits and Systems for Video Technology*, vol. 33, no. 11, pp. 6443-6458, Nov. 2023, doi: 10.1109/TCSVT.2023.3270882.



10.22214/IJRASET



45.98



IMPACT FACTOR:
7.129



IMPACT FACTOR:
7.429



INTERNATIONAL JOURNAL FOR RESEARCH

IN APPLIED SCIENCE & ENGINEERING TECHNOLOGY

Call : 08813907089  (24*7 Support on Whatsapp)